LSS 2018: A DOUBLE-LINED SPECTROSCOPIC BINARY CENTRAL STAR WITH AN EXTREMELY LARGE REFLECTION EFFECT[1]

J. S. Drilling[2,3]

Department of Physics and Astronomy

Louisiana State University

and

Institut für Theoretische Physik und Sternwarte

Universität Kiel

[1]Contributions of the Louisiana State University Observatory No. 000.

[2]Visiting Astronomer, Cerro Tololo Inter-American Observatory, which is operated by the Association of Universities for Research in Astronomy, Inc., under contract with the National Science Foundation.

[3]Guest observer with the International Ultraviolet Explorer Satellite which is sponsored and operated by the National Aeronautics and Space Administration, the Science Research Council of the United Kingdom, and the European Space Agency.

ABSTRACT

LSS 2018, the central star of the planetary nebula DS1, has been found to be a double-lined spectroscopic binary with a period of 8.571 hours. Light variations with the same period have been observed in U, B, and V; in the wavelength regions defined by the two IUE cameras; and in the strength of the CIII 4647 emission line. The light variations can be accurately predicted by a simple 'reflection' effect, and an analysis of the light curves yields the angular diameter and effective temperature of the primary, the radii of the two stars in terms of their separation, and the inclination of the system. Analysis of the radial velocities then yields the masses of the two stars, their separation, the distance of the system, the absolute magnitude of the primary, and the size of the nebula.

I. INTRODUCTION

Bond (1976) and Grauer and Bond (1983) have initiated a search for central stars which show periodic light variations. To date, five new objects have been found, four of which have turned out to be close binaries showing a very large reflection effect. These are the central stars of Abell 41 ($P = 0^d.1132269$; Grauer and Bond 1983), Abell 63 ($P = 0^d.46506918$; Bond, Liller, and Mannery 1978), Abell 46 ($P = 0^d.4717294$; Kurochkin 1980); and K1-2 ($P = 0^d.6707$, Bond 1979). The central stars of Abell 46 (V477 Lyr) and Abell 63 (UU Sge) are also eclipsing binaries, and the light curve of UU Sge has been analyzed by Bond, Liller, and Mannery (1978). The spectrum of the central star of Abell 41 has been discussed by Green, Liebert, and Wesemael (1984). Because of the lack of fundamental mass and radius determinations for central stars, it would be of great importance to establish accurate radial velocity curves for these systems and to obtain time-resolved observations in the ultraviolet, where most of the observable radiation is being emitted. Because of the faintness of these objects ($B > 15$), and their short periods, this has not been done.

Drilling (1983) has discovered 12 new sdO stars, 3 of which have subsequently been found to possess planetary nebulae of low surface brightness. Because these objects are all brighter than $B = 13$ and had not been observed previously, the writer monitored them for light variation during the nights of 1984 April 3 through 10 using the 0.9-meter telescope at Cerro Tololo. Only one, LSS 2018, was found to

vary, and subsequent time-resolved spectroscopic observations were made at high resolution with the 4-meter echelle spectrograph at Cerro Tololo and at low resolution with the IUE satellite. These observations are described and analyzed for the relevant stellar masses and radii below. In all cases, the observations have been phased using a period of 8.571 hours with phase zero (maximum light) occurring at (heliocentric) J. D. 2445796.671.

II. OBSERVATIONS

a) UBV Photometry

Photoelectric UBV measurements of LSS 2018 were made with the 0.9-meter telescope at Cerro Tololo on the nights of 1984 April 3 through 10 using a standard photometer and filters. The reduction procedure outlined by Schulte and Crawford (1961) was used with the following mean extinction coefficients: $\underline{k}$ = 0.16, $\underline{k_1}$ = 0.09, $\underline{k_2}$ = -0.03, $\underline{k_3}$ = 0.31, and $\underline{k_4}$ = 0.01. Transformation coefficients were determined from 37 observations of standard stars for which magnitudes and colors are given by Graham (1982). Night corrections determined from frequent observations of a comparison star located 6.1 E and 1.6 N of LSS 2018 were applied to all observations of LSS 2018. The average $\underline{V}$ magnitude and colors of the comparison star are $\underline{V}$ = 10.87, $\underline{B-V}$ = 0.56, and $\underline{U-B}$ = 0.07. The results for LSS 2018 are shown as squares in Fig. 1. Also shown in Fig. 1 (as crosses) are some very accurate observations of LSS 2018 made using the $\underline{B}$ filter alone. Each point represents the average of as many as 400 five-second integrations made during the nights of 1984 April 5 and April

10. The scatter of the individual observations about the mean light curve is random with a standard deviation of ±0.02.

b) IUE Spectrophotometry

Low-resolution (6 Å) IUE observations were made with both the LWP and SWP cameras during 1984 May 20 and 21. These observations were reduced by the staff at Goddard Space Flight Center using the software described by Turnrose and Thompson (1984). The quantities plotted in Fig. 1 are the total fluxes observed in the wavelength intervals 1240-1945 Å (SWP) and 1945-3120 Å (LWP), corrected for a reddening of $E(B-V) = 0.15$ (Schönberner and Drilling 1984) according to the reddening law of Seaton (1979). Also plotted as B magnitudes in Fig. 1 are the FES (fine error sensor) readings from IUE, shifted vertically so as to give the best fit to the B magnitudes obtained at Cerro Tololo. Because the sensitivity function of the FES is intermediate to those of the Johnson B and V filters (Holm and Rice 1981), and because the variation in $B-V$ over one cycle is negligible, the coincidence of the two sets of observations shows that the light variations remained strictly periodic during the six weeks which elapsed between the photometric observations made at Cerro Tololo and those made with IUE.

c) High-Resolution Spectroscopy

High-resolution (0.3 Å) observations of LSS 2018 giving 70% coverage of the wavelength interval from 4600 to 4900 Å were made with the 4-meter echelle spectrograph and SIT-vidicon detector at Cerro Tololo during the nights of 1984 April 13 and 14. The exposure

time was 30 minutes in all cases. After removal of the fixed pattern noise, the background-subtracted intensities for LSS 2018 were divided by those for a quartz comparison lamp, and then corrected for the mean atmospheric extinction derived above. The spectra were wavelength calibrated using ThA comparison spectra obtained immediately before and after each observation.

The flux in the CIII 4647 emission line, in units of the continuum flux in a 3.4 Å band underlying this line at minimum light, is plotted in Fig. 1. The plotted points (squares) show that the strength of the CIII 4647 emission varies in phase with that of the continuum, and that it disappears completely at minimum light. The heliocentric radial velocity given by the CIII 4647 emission line is plotted in Fig. 2 (squares), as is that given by the He II 4686 absorption line (triangles). It is seen that these observations can be fit quite well by sine curves of amplitude 148 km/sec and 74 km/sec, respectively, with phases π and 0, respectively, at maximum light. The best fit is obtained for a system velocity of -25 km/sec.

III. ANALYSIS

The observations are well explained using the model applied by Grauer and Bond (1983) to the central star of Abell 41, in which a cool star (from which we see only 'reflected' radiation) orbits a very hot subdwarf (which heats both the planetary nebula and the facing hemisphere of the cooler companion). The symmetry of the radial velocity and light curves are well understood if the orbits are circular, the CIII 4647 emission is produced in the atmosphere of

the secondary, and the HeII 4686 absorption is produced in the atmosphere of the primary. A small contribution to the HeII 4686 line by the secondary may be present near maximum light, when the contribution of the secondary to the spectrum as a whole is greatest according to this model.

CIII 4650-51 (two blended lines) and NIII 4641-42 (near the end of one of the echelle orders) are also present in emission, and both the strengths and radial velocities vary in phase with the CIII 4647 emission. NV 4603 and 4619 are weakly present in absorption and show the same radial velocity variations as HeII 4686. The Hβ profile is very complex, but appears to consist of the following: (a) an absorption component of constant strength which shows the same variations in radial velocity as HeII 4686, (b) a second absorption component which varies in strength and radial velocity like the CIII 4647 emission, and (c) an emission core of constant strength whose radial velocity is equal to the system velocity (-25 km/sec). HeII 4686 and CIII 4647 were chosen to define the radial velocity curves because they are the only strong, unblended lines which lie near the centers of the observed echelle orders.

If we assume that the continuous spectrum of the primary is that observed at minimum light (justified by the disappearance of all spectral features varying in phase with the CIII 4647 emission at this time), and that all radiation from the primary which is incident upon the secondary is absorbed and re-emitted according to Planck's law, then we can use Tables I and III of Napier (1968) to reproduce

the first five light curves in Fig. 1, given the radii of the two stars relative to their separation, the inclination of the orbital plane to the plane of the sky, and the effective temperature of the primary. These tables take fully into account the effects due to the finite sizes and separations of the two components. The curves given in Fig. 1 were obtained using 0.12 and 0.18 for the radii of the primary and secondary, respectively, in terms of their separation; an inclination of 72° (for which the system just misses eclipse); and an effective temperature of 77,000 K for the primary.

The effective temperature of 77,000 K for the primary was obtained using R, the ratio of the dereddened flux received by the short-wavelength IUE camera (1240 - 1945 Å) to that received by the long-wavelength camera (1945 - 3120 Å), at minimum light. Schönberner and Drilling (1984) have shown this quantity to be sensitive to the effective temperature, but to be relatively insensitive to interstellar reddening, surface gravity, and composition for $n(He)/n(H) \lesssim 30\%$, and have calibrated R against effective temperature using both model atmospheres and stars whose effective temperatures have been determined by other methods. The goodness of fit of a 77,000 K model to the dereddened energy distribution of LSS 2018 near minimum light may be judged from Fig. 3 of Schönberner and Drilling (1984). The corresponding angular radius for the primary is $1''.5 \times 10^{-6}$.

Numerical experimentation shows that the amplitudes and shapes of the light curves are not very sensitive to the effective temper-

ature of the primary, but that they are extremely sensitive to the stellar radii, and that a change of only 5% in the radius of either star causes a noticeable departure from the observations. The light curves are not very sensitive to the inclination of the system for i > 53°, but cannot be fit at all for i < 53°. The light curves also cannot be fit if Kurucz's (1979) model atmospheres with log g = 4.5 and solar composition are substituted for Planck's law in computing the spectrum of the secondary, as they predict a much larger Balmer jump than that which is observed. The use of these models is, however, unrealistic, as they assume that the atmosphere of the secondary is being illuminated from the inside rather than from the outside, as is the actual case. It would therefore be of interest to compute models with the appropriate boundary conditions, in order to try to predict the line spectrum and to see why the continuous spectrum of the secondary obeys Planck's law so well.

The solid curve fit to the points representing the CIII 4647 emission line strength in Fig. 1 was obtained by scaling the curve for the B magnitudes down to the observed amplitude for the CIII 4647 emission. The dotted curve is the best fit made on the assumption that the hemisphere of the secondary facing the primary is uniformly illuminated by the CIII emission. It is seen that the second curve gives a better fit to the observations than the first. If we decrease the inclination of the system from 72° to 53°, the strength of the CIII emission predicted by the dotted curve at minimum light increases to 20% of its strength at maximum light. Since neither

this nor an eclipse is observed, we conclude that the inclination of the system lies between 53° and 72°.

A complication arises in analyzing the radial velocity curve of the secondary because, according to the model employed, the center of light for the CIII emission and the center of mass of the secondary do not coincide at quarter phase. However, it can easily be shown that the separation of these two points is 0.424 times the radius of the secondary if the hemisphere facing the primary is uniformly illuminated by the CIII emission. If we assume synchronous rotation for the secondary, we then have from the amplitudes of the radial velocity curves:

$$r_b \sin i = 361{,}000 \text{ km, and}$$

$$(r_r - 0.424\ R_r) \sin i = 725{,}000 \text{ km,}$$

where r_b and r_r are the distances of the primary and secondary, respectively, from the center of mass of the system; R_r is the radius of the secondary; and i is the inclination of the orbit. Application of Kepler's Third Law then gives 0.4 M_o (for the primary) and 0.2 M_o (for the secondary) as lower limits on the masses (i = 72°). The corresponding upper limits (for i = 53°) are 0.7 M_o (for the primary) and 0.3 M_o (for the secondary). The separation of the two components must lie between 0.008 and 0.010 AU, and the radii of the two stars are 0.2 - 0.3 R_o (primary) and 0.3 - 0.4 R_o (secondary). Comparison of the angular and linear radii of the primary yields 650 to 800 pc as the distance to the system, and an angular diameter of 180" for the planetary nebula (Drilling 1983) then gives 0.6 to 0.7 pc as its

linear diameter. The corresponding absolute magnitude for the primary (minimum light) is M_V = 2.3 to 2.7.

IV. DISCUSSION

The reflection effect for LSS 2018 is one of the most pronounced such effects observed to date. The fact that the light variation can be predicted so well over such a large range in wavelength using the simplest possible assumption, that all radiation incident on the secondary is absorbed and re-radiated according to Planck's law, is remarkable. It should be pointed out, however, that the masses derived above are, to a large extent, independent of this assumption. This is important, because LSS 2018 is the only double-lined spectroscopic binary known among the central stars, and because such strong constraints can be put on the inclination of this system, we have been able to make the first direct determination of the mass of a central star.

If we plot LSS 2018 in Fig. 7 of Schönberner (1981), in which post-AGB evolutionary tracks for central stars are plotted in the M_V-nebular radius plane (assuming a constant expansion velocity of 20 km/sec), we find that the mass of the primary must be 0.57 $M_\odot$ in order to be consistent with evolutionary theory. This is near the mid-point of the range in masses derived above, and our results thus support Schönberner's conclusion that the mass distribution of central stars has a very sharp peak around 0.58 solar masses.

The masses and radii derived above for the secondary put it on or slightly above the mass-radius relation for main-sequence stars

given by Ritter (1982), which is based on data given by Popper (1980). As pointed out by Ritter (1982), this produces a problem in trying to explain the present state of the system as the result of common-envelope binary evolution, as the secondary has not had time to lose the required amount of mass and come back into thermal equilibrium since the ejection of the observed planetary nebula.

According to the formula given by Kraft, Mathews, and Greenstein (1962), the period of LSS 2018 should be decreasing at the rate of 1-3 x 10^{-5} days per century due to gravitational radiation. This will cause the secondary to fill its Roche lobe in 1-3 x 10^{10} years. Since the primary will evolve into a white dwarf in a much shorter time than this, a cataclysmic binary will be produced. This may happen in a much shorter time if the system can find an additional means of losing angular momentum, such as the magnetic braking discussed by Verbunt and Zwaan (1981). Since the phase shift due to gravitational radiation will amount to 50-100 seconds in 500 years, the matter can eventually be settled by careful monitoring of the light variations.

ACKNOWLEDGEMENTS

I am especially grateful to J. Baldwin of the Cerro Tololo Inter-American Observatory for his help in obtaining and reducing the high-resolution spectra of LSS 2018 described above. I would also like to thank H. Bond, G. Chanmugam, U. Heber, K. Hunger, R. Kudritzki, A. Grauer, A. Landolt, H. Ritter, D. Schönberner, J. Tohline, and A. Uomoto for useful discussions. This research was supported by NSF grants AST 8018766 and INT 8219240, and by NASA grant NAG 5-71.

REFERENCES

Bond, H. E. 1976, Publ. Astron. Soc. Pacific 88, 192.

Bond, H. E. 1979, Dwarfs and Variable Degenerate Stars (IUE Colloquium No. 53, ed. H. M. van Horn and V. Weidemann), p. 266.

Bond, H. E., Liller, W., and Mannery, E. J. 1978, Astrophys. J. 223, 252.

Drilling, J. S. 1983, Ap. J. (Letters) 270, L13.

Graham, J. A. 1982, Publ. Astron. Soc. Pacific 94, 244.

Grauer, A. D., and Bond, H. E. 1983, Astrophys. J. 271, 259.

Green, R. F., Liebert, J., and Wesemael, F. 1984, Astrophys. J. 280, 177.

Holm, A., and Rice, G. 1981, IUE NASA Newsletter No. 15, 74.

Kraft, R. P., Mathews, J., and Greenstein, J. 1962, Astrophys. J. 136, 312.

Kurochkin, N. E. 1980, Astr. Tsirk. No. 1143.

Kurucz, R. L. 1979, Astrophys. J. Suppl. 40, 1.

Napier, W. McD. 1968, Astrophys. Space Sci. 2, 61.

Popper, D. 1980, Ann. Rev. Astron. Astrophys. 18, 115.

Ritter, H. 1982, Proceedings of workshop on "High-Energy Astrophysics", Nanking.

Schönberner, D. 1981, Astron. Astrophys. 103, 119.

Schönberner, D., and Drilling, J. S. 1984, Ap. J. 278, 702.

Schulte, D. H., and Crawford, D. L. 1961, Kitt Peak National Observatory Contribution No. 10.

Seaton, M. J. 1979, Mon. Not. Royal Astron. Soc. 197, 241.

Turnrose, B. E., and Thompson, R. W. 1984, International Ultraviolet Explorer Image Processing Information Manual, Version 2.0, Computer Sciences Corporation, CSC/TM-84/6058.

Verbunt, R., and Zwaan, C. 1981, Astron. Astrophys. 100, L7.

FIGURE CAPTIONS

Figure 1. (a) 13.755 - V. (b) 13.435 - B. (c) 11.885 - U. (d) 2.5 log f_1 + 22.62, where f_1 is the total (dereddened) flux received between 1945 A and 3120 A. (e) 2.5 log f_2 + 21.21, where f_2 is the total (dereddened) flux received between 1240 A and 1945 A. (f) 2.5 log (f_3/f_4 + 1) + 0.25, where f_3 is the total flux of CIII 4647 emission received and f_4 is the total flux received in a 3.4 A band of underlying continuum at minimum light. The squares represent observations made from the ground and the triangles, IUE observations. Open and closed symbols represent observations made on different nights or during different IUE shifts. Crosses represent very accurate photometric observations made using the B filter alone (averages over 1000 second intervals and two different nights). The curves are explained in the text.

Figure 2. (a) Heliocentric radial velocities for LSS 2018 given by the CIII 4647 emission line (squares) compared to a sine curve of amplitude 148 km/sec and phase shift π with respect to maximum light. (b) Heliocentric radial velocities for LSS 2018 given by the HeII 4686 absorption line (triangles) compared to a sine curve of 74 km/sec amplitude and zero phase shift. The system velocity is assumed to be -25 km/sec in both cases. Open symbols represent observations made on April 12, and closed symbols, April 13.

Author's Address: J. S. Drilling

Department of Physics and Astronomy

Louisiana State University

Baton Rouge, LA 70803-4001

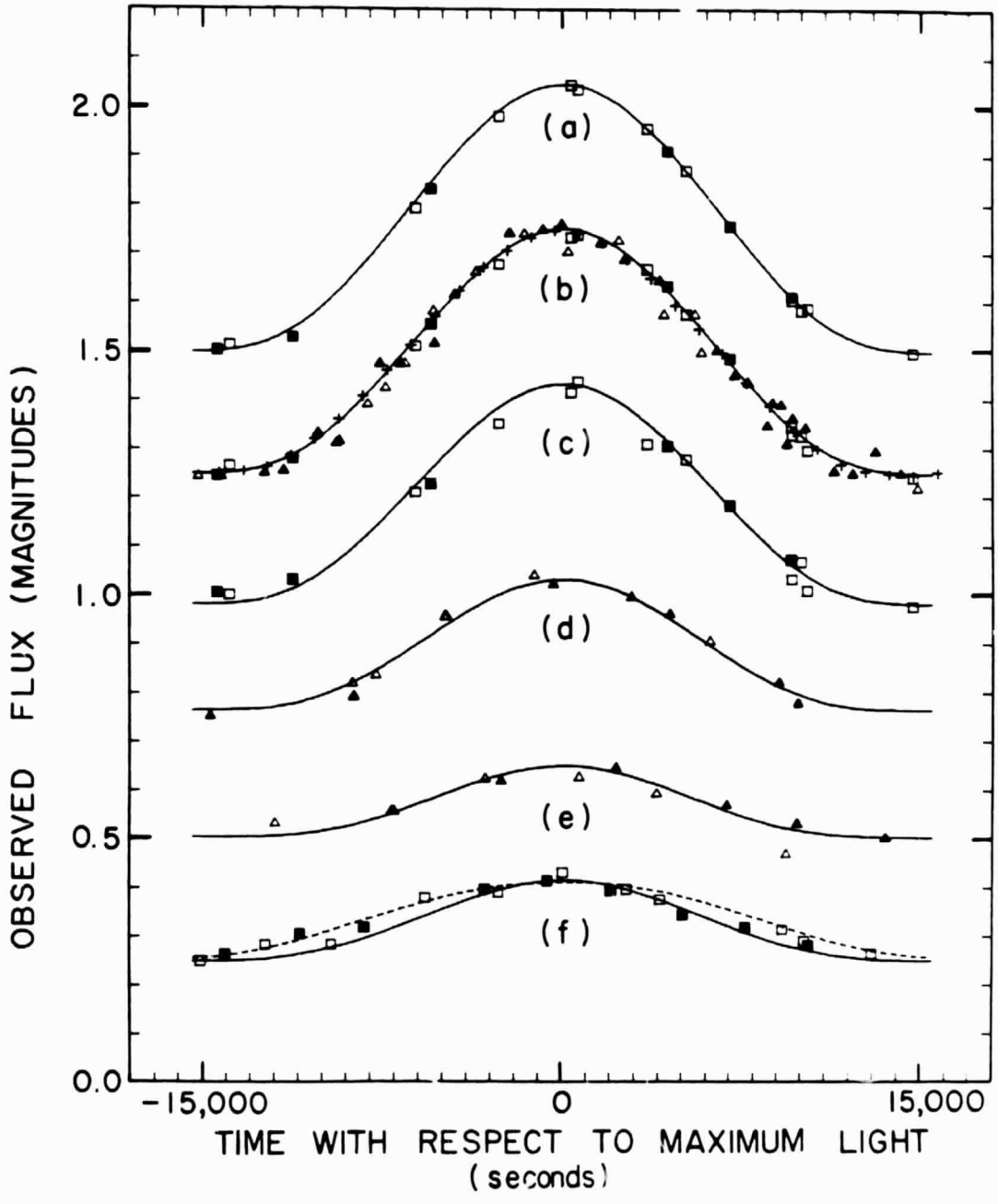
2.0
1.5
1.0
0.5
0.0
(a)
(b)
(c)
(d)
(e)
(f)
OBSERVED FLUX (MAGNITUDES)
-15,000
0
15,000
TIME WITH RESPECT TO MAXIMUM LIGHT
(seconds)

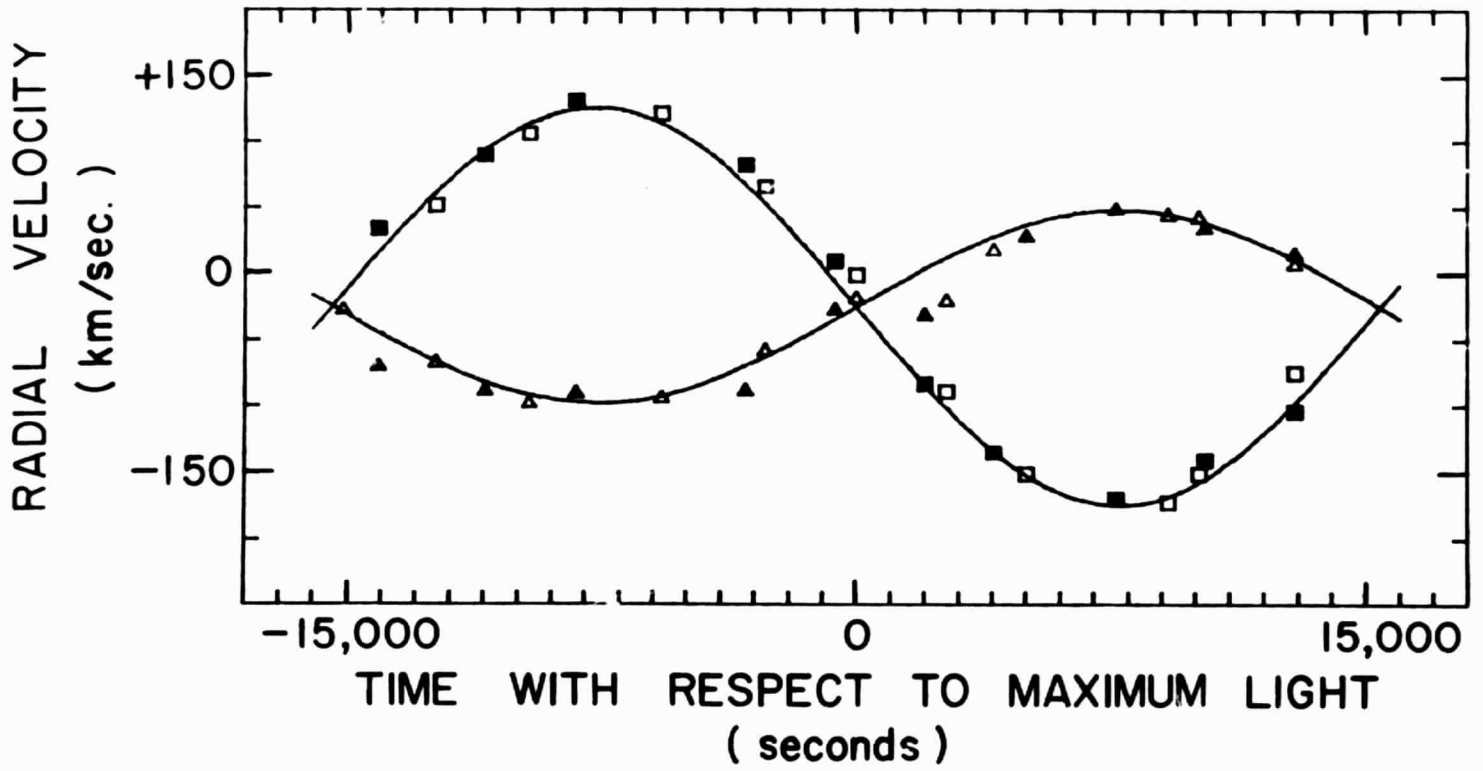
RADIAL VELOCITY
(km/sec.)
+150
0
−150
−15,000
0
15,000
TIME WITH RESPECT TO MAXIMUM LIGHT
(seconds)